PERGAMON Computers and Mathematics with Applications 38 (1999) 245–249

An International Journal
computers & mathematics
with applications

www.elsevier.nl/locate/camwa

The Relation Between Numerical and Material Stress States

H. VAN DER VEEN
Delft University of Technology
Koiter Institute Delft, Faculty of Civil Engineering and Geosciences
P.O. Box 5048, 2600 GA, Delft, The Netherlands

K. VUIK
Delft University of Technology
Faculty of Information Technology and Systems, Department of Applied Mathematics
P.O. Box 356, 2600 AJ, Delft, The Netherlands

R. DE BORST
Delft University of Technology
Koiter Institute Delft, Faculty of Civil Engineering and Geosciences
P.O. Box 5048, 2600 GA, Delft, The Netherlands

Abstract—In a previous article [1], the eigenvalues of the elasto-plastic material matrix of a Drucker-Prager nonassociated soil model were analyzed with special attention to the occurrence of complex eigenvalues. The link between this analysis on material level to stress states which arise in a numerical computation is made in this article. © 1999 Elsevier Science Ltd. All rights reserved.

Keywords—Elasto-plasticity, Eigenvalues, Stresses, Plane-strain, Orthotropy.

1. INTRODUCTION

The relation between stresses and strains is set by the elasto-plastic material matrix. Complex eigenvalues of this matrix may cause difficulties in a numerical analysis. In previous work [1], the eigenvalues of the elasto-plastic material matrix were analyzed for orthotropic and isotropic plane-stress and plane-strain configurations. We found that for isotropic materials the eigenvalues of the elasto-plastic matrix, set up with the Drucker-Prager yield function and a nonassociated flow rule, are always real. However, for orthotropic materials complex eigenvalues have been found. Here, we investigate how stresses that cause complex eigenvalues in the material matrix relate to stresses computed in a numerical analysis.

First, the previous work [1] is summarized in Section 2. In Section 3, the computational setup for a comparison with numerical computations is described. In the last section (Section 4), the stress states arising in three different examples of soil deformation are related to the stress states that lead to complex eigenvalues of the material matrix. The examples discussed are for orthotropic plane-strain materials with no contraction.

The numerical computations are performed with the finite element package DIANA [2] that is maintained and developed at TNO Building and Construction Research, Rijswijk, The Netherlands.

0898-1221/99/$ - see front matter. © 1999 Elsevier Science Ltd. All rights reserved. Typeset by AMS-TEX
PII: S0898-1221(99)00279-5

2. EIGENVALUES OF THE MATERIAL MATRIX

A constitutive law describes the relation between stresses σ and strains ϵ. The elastic response is described by Hooke's law: $\sigma = \mathbf{D}_e\epsilon$, whereas the total elasto-plastic response is given by

$$\dot{\sigma} = \mathbf{D}_{\text{ep}}\dot{\epsilon}, \qquad \mathbf{D}_{\text{ep}} = \mathbf{D}_e - \frac{\mathbf{D}_e\mathbf{m}\mathbf{n}^\top\mathbf{D}_e}{H + \mathbf{n}^\top\mathbf{D}_e\mathbf{m}}, \tag{1}$$

in which H is a hardening parameter. The two vectors $\mathbf{m}$ and $\mathbf{n}$ are the direction of plastic flow and the normal to the yield surface, respectively. The Drucker-Prager yield surface is used to separate the stress states that lead to an elastic response from those that result in plastic deformation. The Drucker-Prager yield function reads

$$f(\sigma_i) = \sqrt{I_1^2 - 3I_2} + \frac{6\sin\phi}{3 - \sin\phi}p - \frac{6c\cos\phi}{3 - \sin\phi} = 0. \tag{2}$$

I_1, I_2 are the first and second invariant of the stress matrix and are functions of σ_i, whereas $p = I_1/3$ is the hydrostatic pressure [2]. Parameters c and ϕ are material parameters, namely the cohesion and the friction angle. The normal to the yield surface $n_i = \frac{\partial f}{\partial \sigma_i}$ changes with a change in friction angle ϕ. The components of the direction of plastic flow are obtained from $m_i = \frac{\partial g}{\partial \sigma_i}$, with g as f but with ϕ replaced by the dilatancy angle ψ of the material. If $\phi = \psi$ the normal to the yield surface equals the direction of plastic flow. Normally, soil is described better with a nonassociated flow rule, i.e., $\phi \neq \psi$ and $\mathbf{D}_{\text{ep}}$, is therefore, nonsymmetric.

In previous work [1], the eigenvalues of the elasto-plastic material matrix $\mathbf{D}_{\text{ep}}$ have been investigated for plane-stress and plane-strain orthotropic and isotropic materials. For orthotropic materials (with no elastic contraction) complex eigenvalues were found for certain stress states. We review briefly an example of an orthotropic plane-strain configuration. For a plane-strain configuration the first and second invariants of the stress matrix read [3]

$$I_1 = \sigma_{xx} + \sigma_{yy} + \sigma_{zz}, \qquad I_2 = \sigma_{xx}\sigma_{yy} + \sigma_{yy}\sigma_{zz} + \sigma_{xx}\sigma_{zz} - \sigma_{xy}^2, \tag{3}$$

and $\mathbf{n}$ is found by taking the appropriate derivatives of the yield function. Because elastic contraction is not included ($\nu = 0$), the elasticity matrix $\mathbf{D}_e$ is diagonal. The diagonal entries of $\mathbf{D}_e$ are the stiffness parameters for different orthogonal directions and the shear modulus. These are chosen equal 55, 60, 50, and 30 N/mm^2, respectively. The cohesion is chosen equal to 0.0001 N/mm^2 and $\sin\phi = 0.3$.

As a ring of the Drucker-Prager yield surface in three dimensions (a cone), we consider the circle that lies in the plane that has the hydrostatic axis as its normal. On the ring, the first and second invariant of the stress matrix are constant [4]. The eigenvalues of $\mathbf{D}_{\text{ep}}$ are computed by varying σ_{xx} and σ_{yy} within the limit given by a fixed I_1. The stress component σ_{zz} then follows from this value of I_1 and with the Drucker-Prager yield function (equation (2)) the second variant I_2 can be obtained as well as σ_{xy}. Figure 1 is a plot of the three nonzero eigenvalues of $\mathbf{D}_{\text{ep}}$ for $I_1 = 0$, where the holes denote complex eigenvalues that appear in conjugate pairs.

3. LINKING MATERIAL AND NUMERICAL STRESSES

Every intermediate equilibrium of a numerical analysis is defined by a stress state (four stresses in case of a plane strain configuration) and thus, relates to a particular value of I_1. A value of I_1 defines a ring of the yield surface and a ring can be presented by a filled oval in the σ_{xx}, σ_{yy} space. The oval's center is the hydrostatic pressure p and its radius follows from the constraint that σ_{xy}^2 must be positive. We would like to show the whole numerical process in one image, and thus, be able to relate the stress states of a numerical analysis to stresses that lead to complex eigenvalues of the material matrix. Therefore, every stress state of an intermediate equilibrium is mapped

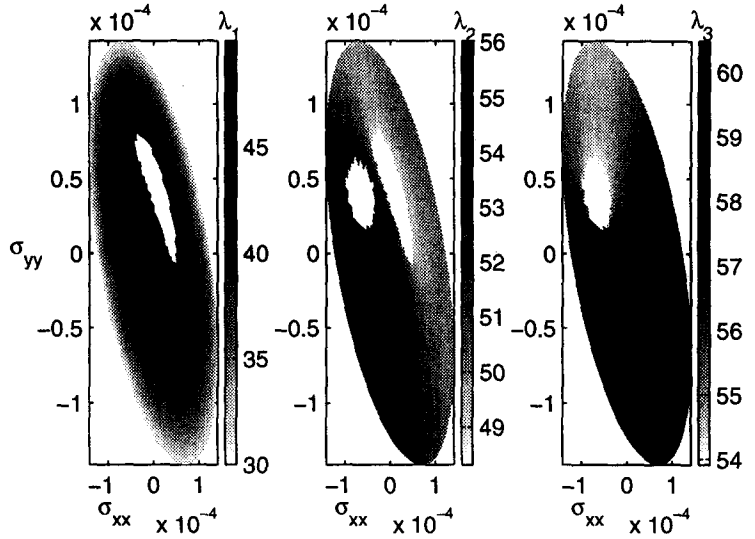

Figure 1. Eigenvalues of the elasto-plastic material matrix. Holes indicate complex eigenvalues.

onto a reference oval defined by $I_1^* = 0$ and $c^* = 0.01$, where the superscript $*$ is used to indicate the reference values. As a consequence $I_2^* = -12c^2\cos^2\phi/(3-\sin\phi)^2$, see also equation (2). The angles ϕ and ψ are fixed during both material and numerical computations and equal 0.3 and 0.1, respectively. With the hydrostatic pressure p as center point, $r(\theta) \in [0, R(\theta)]$ and $\theta \in [0, 2\pi]$ the description of the oval becomes

$$\sigma_{xx} = p + r\cos\theta, \qquad \sigma_{yy} = p + r\sin\theta, \qquad \sigma_{zz} = p - r\sin\theta - r\cos\theta, \tag{4}$$

$$\sigma_{xy}^2 = \sigma_{xx}\sigma_{yy} + \sigma_{xx}\sigma_{zz} + \sigma_{yy}\sigma_{zz} - I_2 = \frac{I_1^2}{3 - I_2} - r^2(1 + \cos\theta\sin\theta). \tag{5}$$

From equation (5), it follows that σ_{xy}^2 attains its maximum at $r = 0$ and vanishes when

$$r = \sqrt{\frac{(I_1^2/3 - I_2)}{(1 + \cos\theta\sin\theta)}} \equiv R, \qquad R^* = \sqrt{\frac{-I_2^*}{(1 + \cos\theta\sin\theta)}}. \tag{6}$$

During the transformation to the reference state p and r change, but we keep θ fixed. In this way, the stress values in the reference state can be computed from an arbitrary stress state via

$$\sigma_{xx}^* = \frac{(\sigma_{xx} - p)R^*}{R}, \qquad \sigma_{yy}^* = \frac{(\sigma_{yy} - p)R^*}{R}, \qquad \sigma_{zz}^* = I_1^* - \sigma_{xx}^* - \sigma_{yy}^*, \tag{7}$$

after which σ_{xy}^* can be computed from I_2^*. The eigenvalues of the elasto-plastic matrix $\mathbf{D}_{\mathrm{ep}}$ are the same in the original state and in the reference state. That is, the normals $\mathbf{m}, \mathbf{n}$ that result in $\mathbf{D}_{\mathrm{ep}}$ are unchanged by the transformation. For example, n_1 is obtained by evaluating $\frac{\partial f}{\partial \sigma_{xx}}$:

$$n_1 = \frac{2I_1^* - 3\sigma_{yy}^* - 3\sigma_{zz}^*}{2\sqrt{(I_1^*)^2 - 3I_2^*}} + C, \tag{8}$$

with $C = 2\sin\phi/(3 - \sin\phi)$. Using equations (6) and (7) and $I_1^* = 0$, it then follows that:

$$n_1 = \frac{-3(\sigma_{yy} + \sigma_{zz} - 2p)\sqrt{-I_2^*}}{2\sqrt{-3I_2^*}\,\sqrt{I_1^2/3 - I_2}} + C, \tag{9}$$

which can be simplified further, using equation (3), such that

$$n_1 = \frac{2I_1 - 3\sigma_{yy} - 3\sigma_{zz}}{2\sqrt{I_1^2 - 3I_2}} + C. \tag{10}$$

Elaborations for n_2, n_3, and n_4 lead to similar relations.

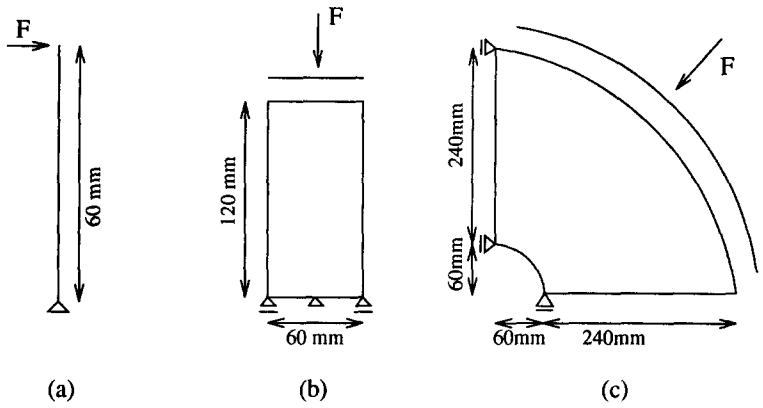

Figure 2. Soil specimen configurations of (a) pure shear, (b) biaxial compression, and (c) borehole stability.

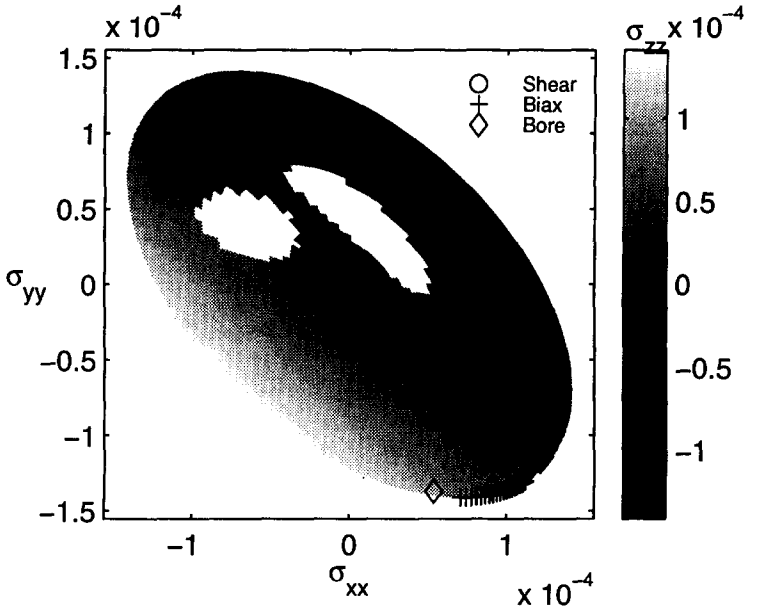

Figure 3. Stress' paths obtained with pure shear (o), biaxial compression (+) and borehole stability (◇), mapped onto stress states of the Drucker-Prager yield surface. Holes denote stress states that yield complex eigenvalues of the material matrix.

4. EXAMPLES

In Section 2, eigenvalues were computed of the plane-strain orthotropic material matrix with material properties that lead to complex eigenvalues. This configuration is chosen as reference state onto which the stress states are mapped of the examples discussed in this section. The numerical computation is continued until the iterative solution procedure for fixed displacement increments [5] fails to converge.

The first example is that of pure shear, see Figure 2. In this test a rod is deformed under shear and is allowed to shorten, but not to bend. The stress states found by the numerical iterative procedure, are mapped onto the reference state according to the procedure described in Section 3. In Figure 3, the absolute value of the shear stress is plotted against the normal stresses σ_{xx}, σ_{yy} for the reference configuration. The holes in the figure denote the areas where at least one of the three eigenvalues of the material matrix is complex (see also Figure 1). Each marker in Figure 3 corresponds to an intermediate equilibrium state of the numerical computation. Even though the stresses lie close to the stress states associated to complex eigenvalues, none of the stresses is actually in this area.

The second example is the biaxial compression test. The specimen is loaded on the top, supported at the bottom, and the sides are free (Figure 2). Because the sides of the specimen are free to move, the shear stress is zero during homogeneous deformation. In Figure 3, the stress path, is therefore, situated on the outer border of the image in the σ_{xx}, σ_{yy} space. As this figure shows, the stresses in this example remain far away from the critical zone.

In the oil industry research is done on the stability of the borehole once the bore is taken out. This is modeled here with a quarter of a horizontal cross section of the soil around the borehole that is loaded on the outer boundary. The computed stresses are situated close to the outer border in Figure 3. There is a large drop in value of the shear stress σ_{xy} near to the side, and the shear stress in this example is of the same order as the normal stresses σ_{xx}, σ_{yy}.

5. CONCLUSION

It was shown how the stresses that yield plastic deformation according to the Drucker-Prager yield function can be related to stress states in a numerical computation. This was done by a visualization in the normal stress space of one particular ring of the Drucker-Prager cone. If two normal stresses are plotted against each other a filled oval evolves. The stresses of the numerical computation were mapped onto this oval and were related to the occurrence of complex eigenvalues of the elasto-plastic material matrix.

The computational setup discussed here provides a link between the stresses of a yield surface and those found in a numerical computation. Stresses for which the constitutive law yields complex eigenvalues in the elasto-plastic material matrix can thus be linked to the outcome of a numerical analysis and to possible computational difficulties. In the three problems discussed here, the stresses found did not coincide with the stress states that lead to complex eigenvalues in the elasto-plastic material matrix but this could happen in other problems.

REFERENCES

1. H. van der Veen, C. Vuik and R. de Borst, An eigenvalue analysis of nonassociated plasticity, *Computers Math. Applic.*, (this issue).
2. F.C. de Witte and P.H. Feenstra, Editors, *DIANA Finite Element Analysis; User's Manual Release 6.1*, TNO Building and Construction Research, The Netherlands, (1996).
3. J. Lubliner, *Plasticity Theory*, Macmillan, New York, (1990).
4. H. van der Veen, The significance and use of eigenvalues and eigenvectors in the numerical analysis of elasto-plastic soils, Ph.D. Thesis, Delft University of Technology, (1998).
5. O.C. Zienkiewicz and R.L. Taylor, *The Finite Element Method*, Fourth Edition, McGraw-Hill, Europe, (1994).